



Nano-Dimensional Elements in the Structure of Zinc Subjected to KOBO Extrusion

Andrzej Korbel¹ · Ludwik Błaż¹ · Włodzimierz Bochniak¹ · Mirosława Pawlyta² · Paweł Ostachowski¹ · Marek Łagoda³

Received: 30 October 2022 / Revised: 10 February 2023 / Accepted: 8 March 2023 / Published online: 24 March 2023
© The Author(s) 2023

Abstract

In the study of plastic flow and mechanical features of zinc subjected to severe plastic deformation at low temperature through the KOBO extrusion method, three techniques of micro and nanostructure identification have been used (TEM, STEM, HAADF). It was shown that the pattern of long trails—a typical element of microstructure after the KOBO deformation, results from strain fields of densely spaced nano-dimensional clusters of point defects—SIA clusters. The presence of satellite spots on the diffraction pattern was explained by a periodic arrangement of clusters which takes the form of a modulated lattice with a nano-sized wavelength.

Keywords Pure zinc · KOBO extrusion · Point defect clusters · Modulated structure

Abbreviations

EDX	Energy dispersive x-ray spectroscopy
FFT	Fast Fourier transform
HAADF	High-angle annular dark field
HRSTEM	High resolution scanning transmission electron microscopy
HRTEM	High resolution transmission electron microscopy
IFFT	Inverse fast Fourier transform
SAD	Selected area diffraction
SIA	Self-interstitial atom
STEM	Scanning transmission electron microscopy
TEM	Transmission electron microscopy

Introduction

Among a variety of plastic deformation methods, the KOBO extrusion enables a particularly big deformation (severe plastic deformation) at low temperatures. Its distinguishable feature is that extrusion is supported by cyclic reversible twisting [1].

The mechanical performance of metals during KOBO deformation and post deformation features of the extrusion products have been the subject of studies reported in a number of papers [1–7]. The discovery that the kinetics of plastic flow in the KOBO extrusion process follows the Newtonian characteristics of viscous liquids (linear relation stress vs. strain rate) was the most important result of these studies. The value of viscosity coefficient in solid metal [1] has to be decreased by several orders through simultaneously increasing the diffusion coefficient [3], where the latter is determined by point defect concentration [3].

This led to a hypothesis that point defects, in particular self-interstitial atoms (SIAs) [2], play a dominant role in the metal's mechanical performance both during and after KOBO extrusion.

The phenomenon was analyzed by a self-consistent model of generation, interaction and annihilation of point defects in the gradient of oscillating stresses [8]. The model proves the existence of a distinct zone of reduced viscosity (zone of intense slip) with sharply increased concentration of point defects—(SIA). Such densely spaced narrow zones appear to

✉ Paweł Ostachowski
pawel.ostachowski@agh.edu.pl

¹ AGH – University of Science and Technology, A. Mickiewicza 30Av., 30-059 Cracow, Poland

² Silesian University of Technology, Konarskiego 18A St., 44-100 Gliwice, Poland

³ Research Network Łukasiewicz – Institute of Non-Ferrous Metals, Sowińskiego St. 5, 44-100 Gliwice, Poland

be typical for the structure of metals after KOBO low temperature deformation [2, 4]. The measurement results of the mechanical performance of metals during extrusion can only be correlated with such elements of structure as point defects and/or their nano-dimension clusters. Unexpected features of the extrusion products such as Lüders deformation in pure metals and superplastic flow in coarse grain materials, provide additional confirmation of the hypothesis [2, 3, 5].

The unusually high strength and ductility of extruded zinc cannot be explained by grain size nor by dislocation density [5], which means that only point defects can be responsible for these properties of zinc. Their experimentally proved thermal stability even after heating to temperature of above $0.7 T_m$ (melting point) [6], would be hard to understand if the defects were separately distributed, therefore it is assumed that they form stable nano-dimensional clusters.

The formation of clusters requires a high concentration of these defects, which can be achieved either by radiation bombardment or by plastic deformation. However, contrary to a somewhat random generation of point defects due to bombardment, their formation and distribution during plastic straining is a derivative of the morphology and orientation of slip zones reflected in the patterns of slip lines [3–5]. Therefore, in the experimental studies we focused on the structure of intense slip zones (shear bands) in metals after low-temperature KOBO extrusion.

Experiment and Results

High purity polycrystalline zinc was used in the experiments. Material purity was confirmed by x-ray spectroscopy method (Table 1) and EDX analyses accompanied by thin foil observations. Transmission electron microscope observations (TEM, HRTEM, HRSTEM and HAADF) of the microstructure of pure zinc (Table 1) after heavy deformation by KOBO extrusion (true strain $\epsilon_r = 3.6$ assisted by reversible torsion by $\pm 8^\circ$ at the frequency of 5 Hz) at room temperature and a constant ram speed of 0.5 mm/s were performed. The KOBO extrusion process was carried out at a deformation ratio $\lambda = 100$, meaning that from a load with the diameter of 40 mm rods with the diameter of 4 mm were obtained.

The samples for structural observations, carried out via both optical microscopy and transmission electron microscopy, were taken according to standard procedures. Mechanically grinded and polished specimens for optical microscopy observations were etched using 10% HNO_3 solution. Thin foils for TEM were electrolytically polished by means of Struers

Tenupol electrolytic device using solution 10 g $\text{AlCl}_3 + 45$ g $\text{ZnCl}_2 + 144$ ml $\text{C}_2\text{H}_5\text{OH} + 32$ ml $\text{H}_2\text{O} + 16$ ml $\text{CH}_3(\text{CH}_2)_3\text{OH}$ and electropolished at $20 \div 25$ V, and 1.5 A/cm^2 current density. A plasma cleaner was used immediately before electron microscopy observations. Structural observations were carried out on the JEOL 2010 field emission transmission electron microscope (TEM) and FEI TITAN 80-300.

An example microstructure of zinc after the KOBO extrusion is presented in Fig. 1. In both cross sections equiaxial grains with the size of around $30 \mu\text{m}$ are visible.

The preliminary TEM observations have shown that the only distinguishable elements of structure in the extruded zinc are long trans-granular trails, such as those shown in Fig. 2a. Figure 2b shows the diffraction (SAD) pattern taken from this area.

The presence of satellites around main diffraction reflections (Figs. 2b and 3a) is a striking feature of the diffraction pattern. Satellites were observed in many grains with different orientations. Their presence implies that there is an “extra order” in the crystalline structure. Inverse fast Fourier

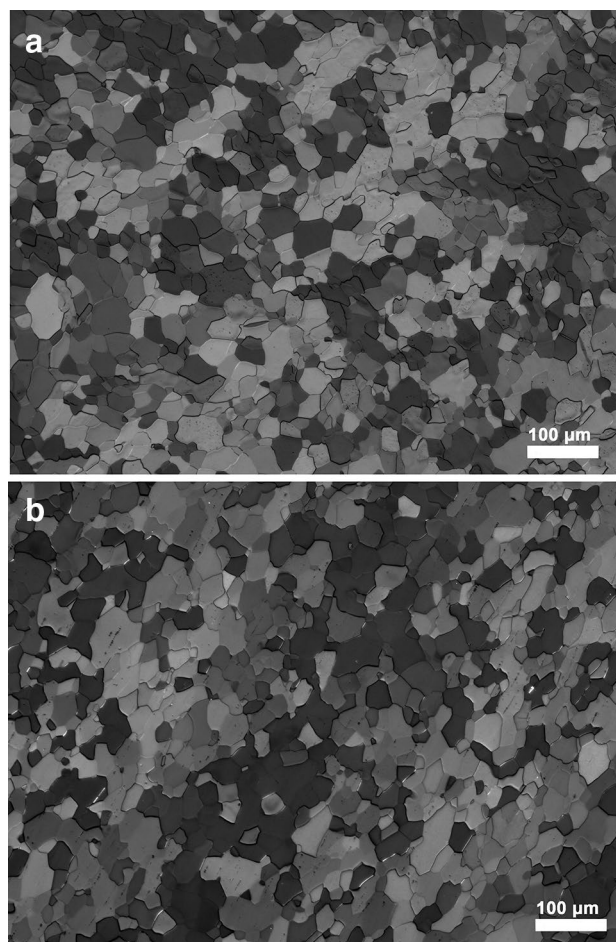


Fig. 1 Optical microscopy microstructure of KOBO-extruded zinc samples observed in transverse (a) and longitudinal (b) cross sections

Table 1 Chemical composition (wt.%) of zinc used for the research

Zn	Pb	Cd	Fe	Cu	Sn
Balance	0.003	0.0001	0.0006	0.0004	0.0001

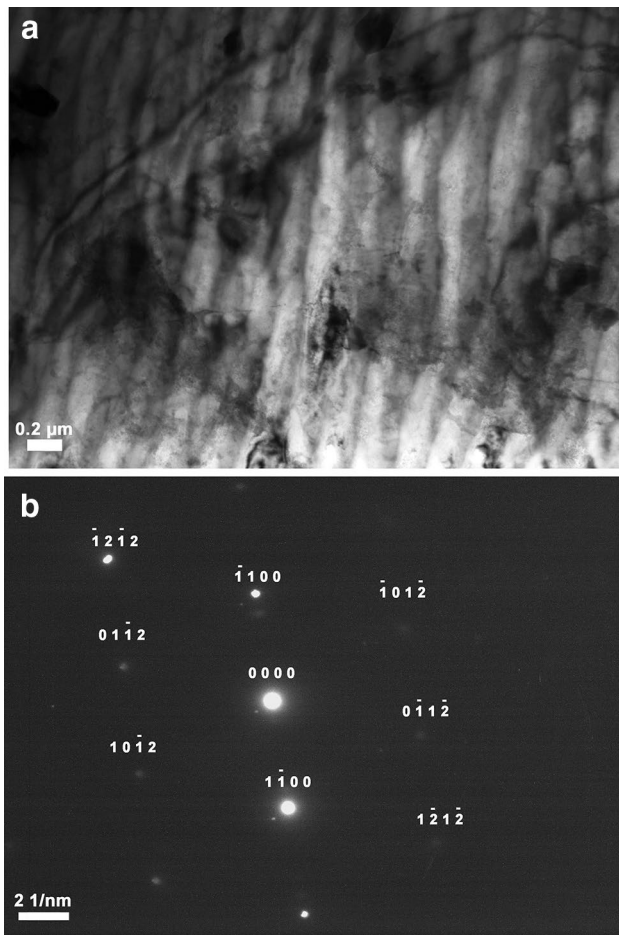


Fig. 2 TEM microstructure (a) of a $\varnothing=4$ mm wire extruded at room temperature by the KOBO method from $\varnothing=40$ mm ingot, as well as a SAD pattern of this area (b)

transform (IFFT) of the diffraction pattern shown in Fig. 3a indicates that some modulation of the zinc crystalline lattice is the source of the satellites (Fig. 3b). An average wavelength of the modulation is about 1.4 nm.

In an attempt to reveal the nature of such an unusual pattern of the crystal structure (particularly in a monoatomic lattice) high resolution observations (HRTEM and HRSTEM) were performed. Figure 3c shows an atom-sized resolution pattern revealed in the area of “trails.” It reveals periodic arrangements of black and white rows with modulation wavelengths of the order of 1.4 nm, which corresponds to that presented in Fig. 3b.

The contrast of the image is not uniform but it is composed of periodically distributed black patches with interpatch distances of the order of 1.4 nm. Apart from the main diffraction spots of zinc lattice, the diffraction image (SAD) contains a symmetrically located “satellite” around each spot in reciprocal lattice distance corresponding to the wavelength of modulation, as shown in Fig. 3b. This

can be treated as evidence of a multi-directional extra order of zinc lattice and of the symmetrical distribution of patches.

Two types of high resolution scanning microscopy—HRSTEM (bright–dark field) and HAADF—used in the study, provided additional information. Figure 4a shows the structure reproduced in the transmission mode of image formation (HRSTEM). The arrangement of patches takes the form of a symmetrical network correlating to the symmetry of the diffraction pattern. In a planar view, black contrast extends across approximately 3–4 atoms within a patch.

Periodic arrangement of the recorded image effects raises the question about their real nature, and specifically whether they are artifacts resulting from the interference of scattered beams—moiré fringes. In the case of the HAADF mode of imaging such an artifact may come exclusively from the interference of the probe with periodically arranged atom columns in the sample, provided that scan spacing is close to the spacing of the specimen lattice (distance between highly localized atomic nuclei) [9].

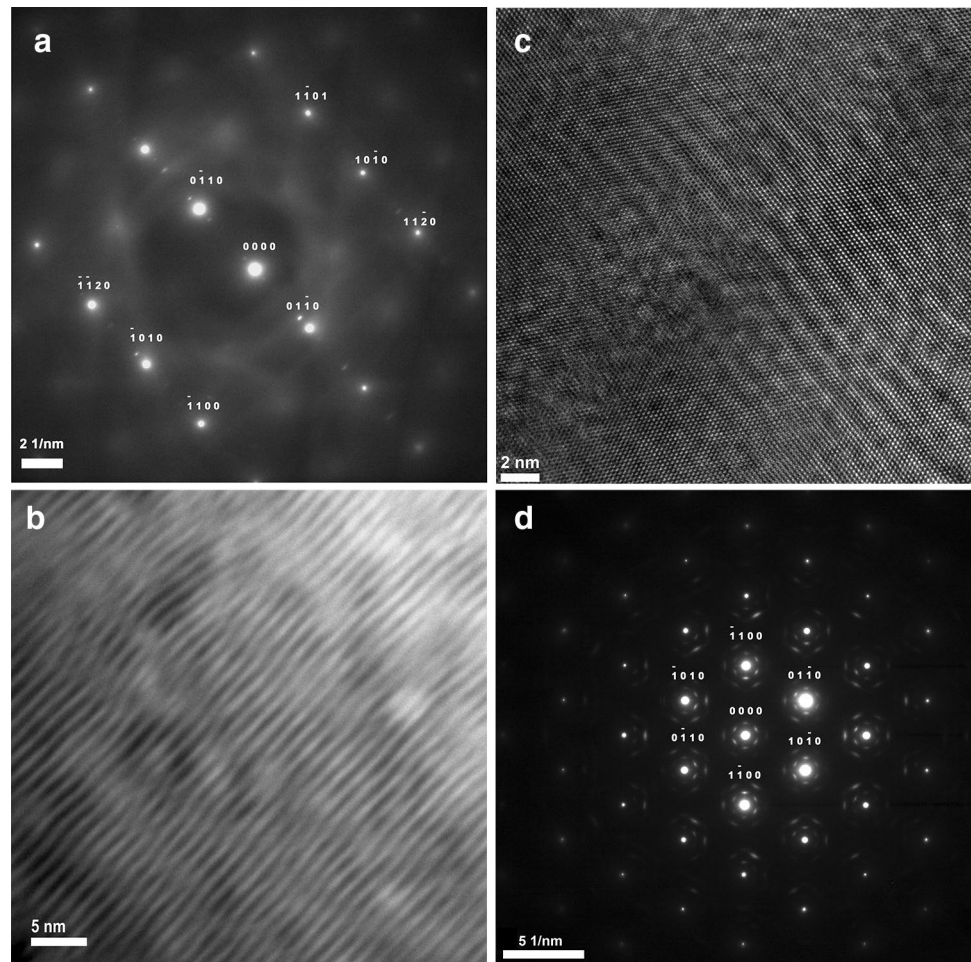
However, this is not the case of the image shown in Fig. 4b. The grating of the scanning probe: 2048×2048 pixels over the sample area 12.6×12.6 nm gives the scan the spacing of 6.15×10^{-3} nm, while the lattice spacing in zinc is 26.1 nm. This means that the scanning probe is taken several times over interatomic distance, which rules out the possibility of the scattered beams interference. Thus the images in Fig. 4 reveal the real structure of zinc.

Figure 5, showing differently oriented colonies of “patches” additionally confirms the above statement.

It is difficult to accurately deduce the structural origin of dark contrast from the STEM image, except that it is formed by coherently scattered electrons (Bragg diffraction). Therefore structural defects responsible for the changes in diffraction conditions—resulting in local distortions, must exist. The size of the distortions reflected in the area of dark contrast allows them to be classified as “point defects.” It is, however, very unlikely for them to be single defects, such as vacancies or self-interstitial atoms (SIAs). Taking the mechanical properties of zinc, as described earlier, into account, it is more probable that stable cluster defects are formed.

The pattern received by HAADF mode of structure imaging supports the suggested interpretation. This is because in the HAADF [9, 10] technique, an image is formed by incoherently scattered electrons (Rutherford scattering by nuclei of the atoms)—as opposed to Bragg scattered electrons. This type of scattering is sensitive to variations of the atomic number of atoms, and, as such, is widely used to identify heavier atoms in the structure. As there are only zinc atoms in the crystal lattice, the differences in the image contrast, such as the ones shown in Fig. 3b, suggest closer distance between scattering centers—atomic nuclei.

Fig. 3 SAD pattern taken from a different grain of the same sample as in Fig. 2a and its IFFT modulated microstructure obtained by inverse fast Fourier transform (b); microstructure (HRTEM) documenting periodic modulation of the crystal lattice (c), and the obtained SAD pattern (d)



The inversion of contrast within the “patches” from dark to bright makes the image shown in Fig. 4 fundamentally different from the others. While the arrangement of patches and inter patch distances are the same, the area of “bright” contrast is focused on 1–3 atoms and frequently takes an orbicular form. Bright atoms in no-central position relative to the symmetrical arrangement of atoms in a patch area can also be observed. Hence, as suggested by the arguments above, the reversal of contrast results from the presence of self-interstitial atom clusters within the illuminated columns of atoms. X-ray spectral analysis (EDX) excludes the role of any other elements than Zn in the structure (Fig. 6).

Summary

All of the performed observations and the plastic flow features of zinc in the KOBO process bring us to a consistent view of the phenomena which lead to the structure formation.

The long trails, considered to be a typical element of structure in metals subjected to KOBO extrusion, which were found in the tested samples result from the change in diffraction conditions (Bragg scattering) caused by densely spaced point defects. This, in turn, indicates that the plastic flow, induced by the KOBO method, generates high concentration of these defects in zones of intense shear (shear bands), as proved by the presence of self-interstitial atoms, identified in the structure (HAADF). The lattice distortion evidenced in diffraction contrast (TEM, STEM) also suggests a high local internal stress associated with these defects. Their high density reinforces the effect and becomes a driving force for stress relaxation—a means of reducing the elastic energy stored in a crystal. It can be expected that this is what the formation of SIA stable clusters leads to. Although the observations do not allow to identify the internal structure of the clusters they lead to two fundamental conclusions. The first one concerns the presence of self-interstitials atoms (SIAs), the role of which, due to their high formation energy, is commonly

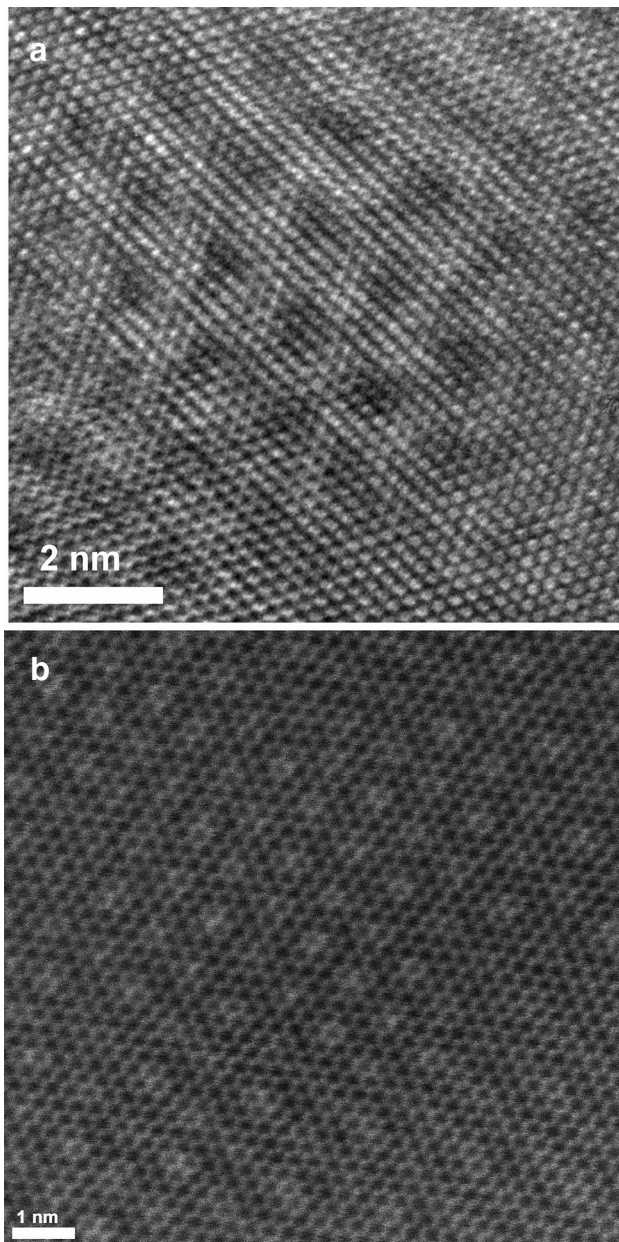


Fig. 4 High resolution STEM (a) and HAADF (b) images of the structure. The samples are the same as in Fig. 3

ignored. In light of the performed experiments and observations they can be produced in large numbers through a change in the dominating slip system (an effect known as strain path change) [2, 3]. A cyclic change of “strain path,” as observed in the KOBO technology, leads to superplastic flow (shear bands) and enables severe plastic formation of metals at low temperatures [7].

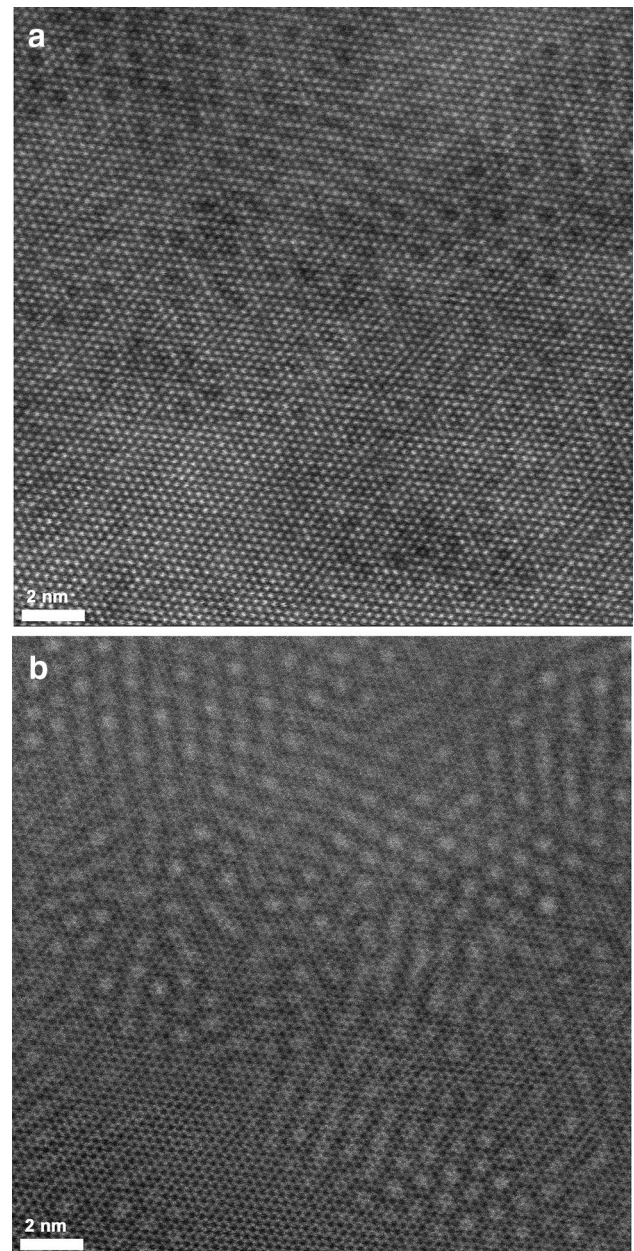


Fig. 5 HRSTEM (a) and HAADF (b) images of the sample nanostructure

The formation of defect (SIA) clusters and their arrangement into nano-dimensional networks in particular, is the second, original and unexpected conclusion. The need to relax internal stresses of defect clusters explains their ordering. The anisotropy of zinc’s elastic properties must be also considered as one of the factors responsible for their internal “construction” and spatial arrangement (super lattice).

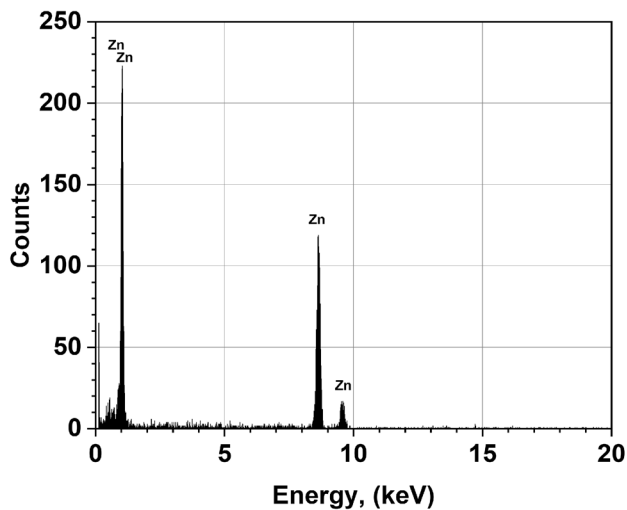


Fig. 6 EDX spectrum received for the material used in investigation

Open Access This article is licensed under a Creative Commons Attribution 4.0 International License, which permits use, sharing, adaptation, distribution and reproduction in any medium or format, as long as you give appropriate credit to the original author(s) and the source, provide a link to the Creative Commons licence, and indicate if changes were made. The images or other third party material in this article are included in the article's Creative Commons licence, unless indicated otherwise in a credit line to the material. If material is not included in the article's Creative Commons licence and your intended use is not permitted by statutory regulation or exceeds the permitted use, you will need to obtain permission directly from the copyright holder. To view a copy of this licence, visit <http://creativecommons.org/licenses/by/4.0/>.

References

1. A. Korbel, W. Bochniak, P. Ostachowski, L. Błaż, Visco-plastic flow of metal in dynamic conditions of complex strain scheme. *Metall. Mater. Trans.* **42A**, 2881–2897 (2011)
2. A. Korbel, W. Bochniak, Lüders deformation and superplastic flow of metals extruded by KOBO method. *Philos. Mag.* **93**, 1883–1913 (2013)
3. A. Korbel, W. Bochniak, Stratified plastic flow in metals. *Int. J. Mech. Sci.* **128–129**, 269–276 (2017)
4. A. Korbel, K. Pięła, P. Ostachowski, M. Łagoda, L. Błaż, W. Bochniak, M. Pawlyta, Structural phenomena induced in course of and post low-temperature KOBO extrusion of AA6013 aluminum alloy. *Mater. Sci. Eng. A.* **710**, 349–358 (2018)
5. A. Korbel, J. Pospiech, W. Bochniak, A. Tarasek, P. Ostachowski, J. Bonarski, New structural and mechanical features of hexagonal materials after room temperature extrusion using the KoBo method. *Int. J. Mater. Res.* **102**, 464–473 (2011)
6. K. Pięła, W. Bochniak, A. Korbel, P. Ostachowski, L. Błaż, Influence of deformation method on structure, mechanical properties and thermal stability of zinc. *Ores Non Ferrous Met.* **54**, 356–360 (2009)
7. A. Korbel, W. Bochniak, Liquid like behavior of solid metals. *Manuf. Lett.* **11**, 5–7 (2017)
8. A. Gusak, M. Danielewski, A. Korbel, W. Bochniak, N. Storozhuk, Elementary model of severe plastic deformation by KoBo process. *J. Appl. Phys.* **115**, 034905 (2015)
9. D. Su, Y. Zhu, Scanning moiré fringe imaging by scanning transmission electron microscopy. *Ultramicroscopy.* **110**, 229–233 (2010)
10. P.D. Nellist, S.J. Pennycook, The principles and interpretation of annular dark-field Z-contrast imaging. *Adv. Imaging Electron Phys.* **113**, 147–203 (2000)

Publisher's Note Springer Nature remains neutral with regard to jurisdictional claims in published maps and institutional affiliations.